GEOPHYSICS, VOL. 88, NO. 5 (SEPTEMBER-OCTOBER 2023); P. C123–C134, 16 FIGS., 1 TABLE.
10.1190/GEO2022-0575.1

Thomsen-type parameters and attenuation coefficients for constant-Q transverse isotropy

Qi Hao[1] and Ilya Tsvankin[2]

ABSTRACT

Transversely isotropic (TI) media with the frequency-independent quality-factor elements (also called "constant-Q" transverse isotropy) are often used to describe attenuation anisotropy in sedimentary rocks. The attenuation coefficients in constant-Q TI models can be conveniently defined in terms of the Thomsen-type attenuation-anisotropy parameters. Recent research indicates that not all those parameters for such constant-Q media are frequency-independent. Here, we present concise analytic formulas for the Thomsen-type attenuation parameters for Kjartansson's constant-Q TI model and show that one of them (δ_Q) varies with frequency. The analytic expression for δ_Q helps evaluate the frequency dependence of the normalized attenuation coefficients of P- and SV-waves by introducing the newly defined "dispersion factors." These factors are frequency-independent and expressed in terms of the Thomsen and Thomsen-type parameters defined at a specified reference frequency. Viscoacoustic constant-Q transverse isotropy is also discussed as a special case, for which the elliptical condition and simplified expressions for the parameters δ and δ_Q are derived. Our results show that, in the presence of significant absorption, the attenuation coefficients of the constant-Q model vary with frequency for oblique propagation with respect to the symmetry axis. This variation needs to be taken into account when applying the spectral-ratio method and other attenuation-analysis techniques.

INTRODUCTION

The frequency-independent quality factor (called constant-Q for brevity) provides a useful phenomenological description of seismic attenuation in rocks and is widely used in seismic attenuation analysis (Barton, 2006). Classic models of this type include the nearly constant-Q model by Kolsky (1956) and the exactly constant-Q model by Kjartansson (1979). For isotropic media, the Kjartansson model produces the constant-Q factor for all frequencies, whereas the Kolsky model leads to nearly constant Q-values. The complex moduli for the Kolsky model represent the first-order Maclaurin series expansion with respect to $1/Q$ of the corresponding moduli for the Kjartansson model (Hao and Greenhalgh, 2021).

As an extension of nonattenuative transverse isotropy, the constant-Q transversely isotropic (TI) model can be used to process seismic attenuation data for most sedimentary rocks, such as shale formations. The constant-Q assumption facilitates the estimation of the quality factor (e.g., Zhang and Ulrych, 2002; Li et al., 2020) and attenuation anisotropy (e.g., Behura and Tsvankin, 2009a; Shekar and Tsvankin, 2011, 2012; Behura et al., 2012). Ultrasonic measurements for rock samples demonstrate that attenuation anisotropy generally is stronger than velocity anisotropy (Best et al., 2007; Zhu et al., 2007; Zhubayev et al., 2016).

Theoretical studies for attenuative anisotropic media include analysis of plane-wave velocities and attenuation (Červený and Pšencík, 2005a, 2005b; Zhu and Tsvankin, 2006; Behura and Tsvankin, 2009c), reflection/transmission coefficients (Carcione, 1997a, 1997b; Behura and Tsvankin, 2009b), point-source radiation (Vavryčuk, 2007a; Shekar and Tsvankin, 2014), and ray-theoretical properties (Vavryčuk, 2007b, 2008; Červený and Pšencík, 2009).

Velocity anisotropy for TI media can be efficiently described by the Thomsen anisotropy parameters (Thomsen, 1986; Tsvankin, 2001). Likewise, attenuation anisotropy for TI media is convenient to study using the Thomsen-type notation introduced by Zhu and Tsvankin (2006). The combination of the velocity- and attenuation-related Thomsen-type parameters (Zhu and Tsvankin, 2006) completely define the complex stiffness matrix at a specified frequency for a general attenuative TI model with a vertical symmetry axis (VTI medium). The generic Thomsen velocity parameters depend

Manuscript received by the Editor 10 September 2022; revised manuscript received 26 March 2023; published ahead of production 15 May 2021; published online 22 June 2023.
[1]Jilin University, College of Geoexploration Science and Technology, Changchun, China. E-mail: xqi.hao@gmail.com (corresponding author).
[2]Colorado School of Mines, Center for Wave Phenomena, Department of Geophysics, Golden, Colorado, USA. E-mail: itsvanki@mines.edu.

on the real parts of the stiffness coefficients (c_{ij}), whereas the Thomsen-type attenuation parameters are defined by the real and imaginary parts of c_{ij}. Hao et al. (2022) find that some Thomsen-type parameters in constant-Q VTI media are frequency dependent. This phenomenon is not entirely surprising because all stiffness coefficients of constant-Q TI media, which are involved in the definition of the Thomsen-type parameters, are functions of frequency. Investigating the frequency variations of these parameters can facilitate the understanding of such key signatures in TI media as velocities, traveltimes, attenuation coefficients, and polarization vectors. However, to our knowledge, there are no analytic expressions for the frequency-dependent Thomsen-type attenuation parameters in constant-Q attenuative VTI media.

The main goal of this paper is to develop analytic expressions for the Thomsen-type parameters and the normalized attenuation coefficients for Kjartansson's constant-Q VTI model. A set of the reference Thomsen and Thomsen-type parameters is defined at a specified frequency and used to obtain those parameters for the entire frequency range. We also present a formula for the frequency-dependent anellipticity and define the condition for elliptical anisotropy in constant-Q TI media. The newly proposed formulas for the Thomsen-type parameters allow us to study the normalized plane-wave attenuation coefficients in constant-Q media with weak attenuation anisotropy and define the dispersion factors for P- and SV-waves. Numerical examples are used to analyze the accuracy of the obtained expressions for the Thomsen-type parameters, the validity of the elliptical condition, and the frequency dependence of the normalized attenuation coefficients.

THOMSEN-TYPE PARAMETERS OF CONSTANT-Q VTI MEDIA

Constant-Q VTI model

Referring to Zhu and Tsvankin (2006) and Carcione (2014), the complex stiffness (or modulus) matrix $\mathbf{M}$ for viscoelastic VTI media is given by:

$$\mathbf{M}=\begin{pmatrix} M_{11} & M_{11}-2M_{66} & M_{13} & 0 & 0 & 0 \\ M_{11}-2M_{66} & M_{11} & M_{13} & 0 & 0 & 0 \\ M_{13} & M_{13} & M_{33} & 0 & 0 & 0 \\ 0 & 0 & 0 & M_{55} & 0 & 0 \\ 0 & 0 & 0 & 0 & M_{55} & 0 \\ 0 & 0 & 0 & 0 & 0 & M_{66} \end{pmatrix}, \tag{1}$$

where $M_{ij}=M_{ij}^R-i\,\mathrm{sgn}(f)M_{ij}^I$ denote the complex stiffness coefficients for the frequency f and the minus sign in front of $i\,\mathrm{sgn}(f)M_{ij}^I$ follows from the definition of the Fourier transform in Červený and Pšencík (2009) and Hao and Greenhalgh (2021). The real and imaginary parts of M_{ij} generally are frequency dependent.

For the Kjartansson's model (also called the constant-Q model), the nonzero independent elements in equation 1 are expressed as (Kjartansson, 1979)

$$M_{ij}=\frac{\tilde{M}_{ij}^R}{\cos(\pi\gamma_{ij})}\left(-i\frac{f}{f_0}\right)^{2\gamma_{ij}}, \tag{2}$$

with

$$\gamma_{ij}=\frac{1}{\pi}\tan^{-1}\left(\frac{1}{Q_{ij}}\right), \tag{3}$$

where $Q_{ij}\equiv M_{ij}^R/M_{ij}^I$, f_0 is the reference frequency, and $\tilde{M}_{ij}^R$ denote the real parts of M_{ij} at f_0: $\tilde{M}_{ij}^R=\mathrm{Re}(M_{ij})|_{f=f_0}$. The reference frequency is set equal to the predominant frequency of the source wavelet (Hao and Greenhalgh, 2021), which is consistent with the choice of f_0 in Bai and Tsvankin (2016), who perform constant-Q anisotropic wavefield modeling using the generalized standard linear solid model. By design, the quality-factor elements Q_{ij} for the Kjartansson model are independent of frequency. As follows from equation 2, the complex stiffness coefficients M_{ij} for a given frequency can be expressed in terms of $\tilde{M}_{ij}^R$ and Q_{ij}.

Thomsen-type parameterization

Attenuative VTI media can be described by the Thomsen (1986) velocity parameters and the Thomsen-type attenuation parameters (Zhu and Tsvankin, 2006; Tsvankin and Grechka, 2011). Note that this notation remains entirely valid in TI media with a tilted symmetry axis (TTI). A complete description of TTI models also requires specifying two angles responsible for the symmetry-axis orientation.

The Thomsen (1986) velocity parameters (see Tsvankin, 2001) are defined in the nonattenuative reference VTI medium. Their definitions in equations 4–8 below follow Tsvankin and Grechka (2011).

The parameter V_{P0} is the vertical velocity of P-waves:

$$V_{P0}\equiv\sqrt{\frac{M_{33}^R}{\rho}}, \tag{4}$$

where ρ denotes density.

The parameter V_{S0} is the vertical velocity of S-waves:

$$V_{S0}\equiv\sqrt{\frac{M_{55}^R}{\rho}}. \tag{5}$$

The parameter ϵ is approximately equal to the fractional difference between the horizontal and vertical velocities of P-waves:

$$\epsilon\equiv\frac{M_{11}^R-M_{33}^R}{2M_{33}^R}. \tag{6}$$

The parameter δ determines the second derivative of the P-wave phase velocity at vertical incidence and is given by:

$$\delta\equiv\frac{(M_{13}^R+M_{55}^R)^2-(M_{33}^R-M_{55}^R)^2}{2M_{33}^R(M_{33}^R-M_{55}^R)}. \tag{7}$$

The parameter γ is approximately equal to the fractional difference between the horizontal and vertical velocities of SH-waves:

$$\gamma\equiv\frac{M_{66}^R-M_{55}^R}{2M_{55}^R}. \tag{8}$$

The Thomsen-type attenuation parameters (Zhu and Tsvankin, 2006) can be used to define the normalized phase attenuation

coefficient $\mathcal{A} \equiv |\mathbf{k}_I|/|\mathbf{k}_R|$ for P-, SV-, and SH-waves, which is generally supposed to be frequency-independent in constant-Q models. For brevity, hereafter $\mathcal{A}$ is called simply the attenuation coefficient. For more details about the coefficient $\mathcal{A}$, see the section "Plane-wave attenuation in constant-Q VTI media" below.

The definitions of the Thomsen-type attenuation parameters, which are given by equations 9–13 below, follow Zhu and Tsvankin (2006).

The parameter $\mathcal{A}_{P0}$ is the vertical attenuation coefficient of P-waves:

$$\mathcal{A}_{P0} \equiv Q_{33}\left(\sqrt{1+\frac{1}{Q_{33}^2}}-1\right) \approx \frac{1}{2Q_{33}}. \tag{9}$$

The parameter $\mathcal{A}_{S0}$ is the vertical attenuation coefficient of S-waves:

$$\mathcal{A}_{S0} \equiv Q_{55}\left(\sqrt{1+\frac{1}{Q_{55}^2}}-1\right) \approx \frac{1}{2Q_{55}}. \tag{10}$$

The parameter ϵ_Q is close to the fractional difference between the horizontal and vertical attenuation coefficients of P-waves:

$$\epsilon_Q \equiv \frac{Q_{33}-Q_{11}}{Q_{11}}. \tag{11}$$

The parameter δ_Q controls the second derivative of the P-wave attenuation coefficient at the vertical incidence and is expressed as:

$$\delta_Q \equiv \frac{\frac{Q_{33}-Q_{55}}{Q_{55}} M_{55}^R \frac{(M_{13}^R+M_{33}^R)^2}{M_{33}^R-M_{55}^R} + 2\frac{Q_{33}-Q_{13}}{Q_{13}} M_{13}^R (M_{13}^R+M_{55}^R)}{M_{33}^R (M_{33}^R-M_{55}^R)}. \tag{12}$$

The parameter γ_Q is close to the fractional difference between the normalized horizontal and vertical attenuation coefficients of SH-waves:

$$\gamma_Q \equiv \frac{Q_{55}-Q_{66}}{Q_{66}}. \tag{13}$$

ANALYTIC DESCRIPTION OF THOMSEN-TYPE PARAMETERS

In this section, we represent the Thomsen velocity parameters and Thomsen-type attenuation parameters in terms of their reference values defined at $f = f_0$: $\tilde{V}_{P0} = V_{P0}|_{f=f_0}$, $\tilde{V}_{S0} = V_{S0}|_{f=f_0}$, $\tilde{\epsilon} = \epsilon|_{f=f_0}$, $\tilde{\delta} = \delta|_{f=f_0}$, $\tilde{\mathcal{A}}_{P0} = \mathcal{A}_{P0}|_{f=f_0}$, $\tilde{\mathcal{A}}_{S0} = \mathcal{A}_{S0}|_{f=f_0}$, $\tilde{\epsilon}_Q = \epsilon_Q|_{f=f_0}$, and $\tilde{\delta}_Q = \delta_Q|_{f=f_0}$. These parameters are used to find the real parts of the reference stiffness coefficients ($\tilde{M}_{ij}^R$), the quality-factor elements Q_{ij} (see Appendix A), and the frequency-dependent stiffness matrix $\mathbf{M}$.

According to equations 4–7 and 12, the Thomsen-type parameters involve the coefficients M_{ij}^R, where ij = 11, 13, 33, 55, and 66. Using equations 2 and 3, M_{ij}^R are approximately expressed as:

$$M_{ij}^R \approx \tilde{M}_{ij}^R\left(1+\frac{2}{\pi}Q_{ij}^{-1}\ln\left|\frac{f}{f_0}\right|+\frac{2}{\pi^2}Q_{ij}^{-2}\ln^2\left|\frac{f}{f_0}\right|\right), \tag{14}$$

where we use the approximation $\tan^{-1}(Q_{ij}^{-1}) \approx Q_{ij}^{-1}$ because typically $Q_{ij} \gg 1$.

Substitution of equation 14 into equations 4–7 and 12 allows us to derive approximate expressions for the frequency-dependent Thomsen and Thomsen-type parameters, which are discussed in the following two subsections.

Velocity parameters

The second-order approximations for the Thomsen velocity parameters with respect to $\ln|f/f_0|$ are given by

$$V_{P0} = \tilde{V}_{P0}\left(1+\frac{1}{\pi}Q_{33}^{-1}\ln\left|\frac{f}{f_0}\right|+\frac{1}{2\pi^2}Q_{33}^{-2}\ln^2\left|\frac{f}{f_0}\right|\right), \tag{15}$$

$$V_{S0} = \tilde{V}_{S0}\left(1+\frac{1}{\pi}Q_{55}^{-1}\ln\left|\frac{f}{f_0}\right|+\frac{1}{2\pi^2}Q_{55}^{-2}\ln^2\left|\frac{f}{f_0}\right|\right), \tag{16}$$

$$\epsilon = \tilde{\epsilon}+\frac{1}{\pi}(1+2\tilde{\epsilon})Q_{33}^{-1}\tilde{\epsilon}_Q\ln\left|\frac{f}{f_0}\right| + \frac{1}{\pi^2}(1+2\tilde{\epsilon})Q_{33}^{-2}\tilde{\epsilon}_Q^2\ln^2\left|\frac{f}{f_0}\right|, \tag{17}$$

$$\delta = \tilde{\delta}+\frac{1}{\pi}Q_{33}^{-1}\tilde{\delta}_Q\ln\left|\frac{f}{f_0}\right|+\frac{1}{\pi^2}Q_{33}^{-2}\zeta_Q\ln^2\left|\frac{f}{f_0}\right|, \tag{18}$$

$$\gamma = \tilde{\gamma}+\frac{1}{\pi}(1+2\tilde{\gamma})Q_{55}^{-1}\tilde{\gamma}_Q\ln\left|\frac{f}{f_0}\right| + \frac{1}{\pi^2}(1+2\tilde{\gamma})Q_{55}^{-2}\tilde{\gamma}_Q^2\ln^2\left|\frac{f}{f_0}\right|, \tag{19}$$

where the P- and S-wave inverse vertical quality factors Q_{33} and Q_{55} (respectively) are:

$$Q_{33}^{-1} = \frac{2\tilde{\mathcal{A}}_{P0}}{1-\tilde{\mathcal{A}}_{P0}^2}, \tag{20}$$

$$Q_{55}^{-1} = \frac{2\tilde{\mathcal{A}}_{S0}}{1-\tilde{\mathcal{A}}_{S0}^2}. \tag{21}$$

The coefficient ζ_Q in equation 18 is defined as:

$$\zeta_Q = d_0(1-g_Q)^2 + d_1(1-g_Q)\tilde{\delta}_Q + d_2\tilde{\delta}_Q^2, \tag{22}$$

with

$$g_Q \equiv \frac{Q_{33}}{Q_{55}}, \tag{23}$$

$$d_0 = \frac{g(1-g+\chi)^2[(1+2\tilde{\delta})\chi-(1+2\tilde{\delta})g+(1+\tilde{\delta})g^2]}{(1-g)^2(\chi-g)\chi^2}, \tag{24}$$

$$d_1 = \frac{2g[1+2\tilde{\delta}+\chi-(2+\tilde{\delta}+\chi)g+g^2]}{(\chi-g)\chi^2}, \tag{25}$$

$$d_2 = \frac{2\chi-g}{2(1+2\tilde{\delta}-g)(\chi-g)}, \tag{26}$$

$$g \equiv \frac{\tilde{V}_{S0}^2}{\tilde{V}_{P0}^2}, \tag{27}$$

$$\chi = \sqrt{(1-g)(1+2\tilde{\delta}-g)}. \tag{28}$$

In equations 15–19, the first-order terms with respect to $\ln|f/f_0|$ are scaled by Q_{33}^{-1} or Q_{55}^{-1}, whereas the second-order terms are scaled by Q_{33}^{-2} or Q_{55}^{-2}. Because Q_{33} and Q_{55} typically are much greater than unity, the frequency dependence of the velocity parameters is mostly determined by the first-order terms. Equations 15–19 indicate that (1) V_{P0} and V_{S0} always monotonically increase with frequency and (2) ϵ, δ, and γ also monotonically increase with f, if $\tilde{\epsilon}_Q > 0$, $\tilde{\delta}_Q > 0$, and $\tilde{\gamma}_Q > 0$, respectively. Overall, the frequency dependence of V_{P0}, V_{S0}, ϵ, δ, and γ for realistic values of Q_{33} and Q_{55} ($Q_{33} \gg 1$ and $Q_{55} \gg 1$) remains weak, as illustrated by the numerical examples below.

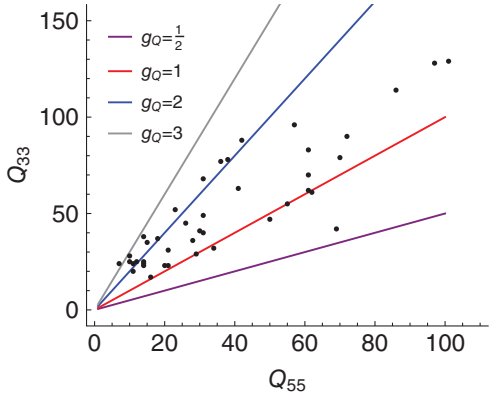

Figure 1. Vertical quality factors Q_{33} and Q_{55} in attenuative VTI rocks. The black dots are the data from Table 3 of Best et al. (2007); $g_Q \equiv Q_{33}/Q_{55}$.

Note that phase and group velocities in strongly attenuative TI media are influenced by attenuation and do not represent the same functions of the Thomsen parameters as in purely elastic models (Tsvankin, 2001; Zhu and Tsvankin, 2006). For sedimentary formations, g_Q and g vary within a limited range. In particular, according to Best et al. (2007), for relatively shallow sedimentary rocks, $0.5 < g_Q \le 3$ (Figure 1).

Using equations 17 and 18 for ϵ and δ, the anellipticity parameter η (Alkhalifah and Tsvankin, 1995) can be approximately obtained as:

$$\eta \equiv \frac{\epsilon-\delta}{1+2\delta} = \eta_0 + \frac{1}{\pi}\eta_1 Q_{33}^{-1} \ln\left|\frac{f}{f_0}\right| + \frac{1}{\pi^2}\eta_2 Q_{33}^{-2}\ln^2\left|\frac{f}{f_0}\right|, \tag{29}$$

where Q_{33} is given by equation 20, and

$$\eta_0 = \frac{\tilde{\epsilon}-\tilde{\delta}}{1+2\tilde{\delta}}, \tag{30}$$

$$\eta_1 = \frac{1+2\tilde{\epsilon}}{(1+2\tilde{\delta})^2}[(1+2\tilde{\delta})\tilde{\epsilon}_Q - \tilde{\delta}_Q], \tag{31}$$

$$\eta_2 = \frac{1+2\tilde{\epsilon}}{1+2\tilde{\delta}}\left[r_0 + \frac{r_1}{1+2\tilde{\delta}} + \frac{r_2}{(1+2\tilde{\delta})^2}\right], \tag{32}$$

with

$$r_0 = \tilde{\epsilon}_Q^2, \tag{33}$$

$$r_1 = -\zeta_Q - 2\tilde{\epsilon}_Q\,\tilde{\delta}_Q, \tag{34}$$

$$r_2 = 2\tilde{\delta}_Q^2. \tag{35}$$

The parameter η controls (along with the zero-dip normal-moveout velocity) all P-wave time-domain signatures for laterally homogeneous VTI media above a horizontal or dipping target reflector (Alkhalifah and Tsvankin, 1995; Tsvankin, 2001).

Attenuation parameters

The following Thomsen-type attenuation parameters are expressed directly through the elements Q_{ij} and, therefore, are frequency-independent in constant-Q VTI media:

$$\mathcal{A}_{P0} = \tilde{\mathcal{A}}_{P0}, \tag{36}$$

$$\mathcal{A}_{S0} = \tilde{\mathcal{A}}_{S0}, \tag{37}$$

DOI:10.1190/geo2022-0575.1

$$\epsilon_Q = \tilde{\epsilon}_Q, \tag{38}$$

$$\gamma_Q = \tilde{\gamma}_Q. \tag{39}$$

The attenuation parameter δ_Q, however, also depends on the coefficients M_{ij}^R (equation 12), which vary with frequency. The second-order approximation for δ_Q with respect to $\ln|f/f_0|$ is:

$$\delta_Q = \tilde{\delta}_Q + \frac{2}{\pi} Q_{33}^{-1} \zeta_Q \ln\left|\frac{f}{f_0}\right| + \frac{2}{\pi^2} Q_{33}^{-2} \xi_Q \ln^2\left|\frac{f}{f_0}\right|, \tag{40}$$

where ζ_Q is defined in equation 22 and

$$\xi_Q = s_0(1-g_Q)^3 + s_1(1-g_Q)^2\tilde{\delta}_Q + s_2(1-g_Q)\tilde{\delta}_Q^2 + s_3\tilde{\delta}_Q^3. \tag{41}$$

The explicit expressions for the coefficients s_i are given in Appendix B.

Because for $Q_{33} \gg 1$ the influence of the second-order term in equation 40 is insignificant, the dependence of δ_Q on frequency is largely controlled by the coefficient ζ_Q. For $\zeta_Q > 0$, δ_Q monotonically increases with frequency. As follows from equations 22 and 24–28, ζ_Q is a function of g (equation 27), g_Q (equation 23), $\tilde{\delta}$, and $\tilde{\delta}_Q$.

Numerical analysis

Here, we analyze the above expressions for the Thomsen-type parameters numerically. The reference frequency is set as $f_0 = 40$ Hz and the frequency range as $[1, 200]$ Hz for all examples below.

First, we test the accuracy of equations 15 and 16 for the vertical velocities and their first-order versions (i.e., those without the second-order term with respect to $\ln|f/f_0|$). As demonstrated in Figure 2, the first-order approximations for V_{P0} and V_{S0} are sufficiently accurate even for strong attenuation in a wide frequency range. Overall, the frequency dependence of the vertical velocities is almost negligible, except for very low frequencies.

Figures 3, 4, and 5 show that the first-order versions of equations 17–19 can accurately describe the variations of the anisotropy parameters ϵ, δ, and γ, respectively, with frequency. Figures 3–5 also confirm that the reference parameters $\tilde{\epsilon}_Q$, $\tilde{\delta}_Q$, and $\tilde{\gamma}_Q$ govern the frequency dependence of ϵ, δ, and γ, respectively. For example, if $\tilde{\epsilon}_Q > 0$, ϵ increases with frequency. As is the case for V_{P0} and V_{S0}, the anisotropy coefficients vary with frequency primarily in the low-frequency range.

Next, we investigate the only frequency-dependent attenuation-anisotropy parameter δ_Q by comparing the exact equation for δ_Q with its first- and second-order approximations. The first-order equation accurately models δ_Q in a wide frequency range, whereas the contribution of the second-order term is practically negligible (Figure 6).

As mentioned above, the coefficient ζ_Q in equation 40 is largely responsible for the frequency variation of δ_Q for a specified value of Q_{33}. Equation 22 shows that ζ_Q is a function of the parameters $g = \tilde{V}_{S0}^2/\tilde{V}_{P0}^2$, $g_Q = Q_{55}^{-1}/Q_{33}^{-1}$, $\tilde{\delta}$, and $\tilde{\delta}_Q$. Using the results from Figure 1, we restrict g_Q to the range $0.5 \le g_Q \le 3$. Figures 7 and 8 show that the smallest absolute value of ζ_Q corresponds to $g_Q = 1$, and $|\zeta_Q|$ increases with the deviation of g_Q from unity. As a result, the parameter δ_Q is almost independent of frequency for $g_Q = 1$ (Figure 9). Overall, the frequency dependence of δ_Q becomes noticeable for large $|g_Q - 1|$ (e.g., $g_Q = 3$; Figure 9),

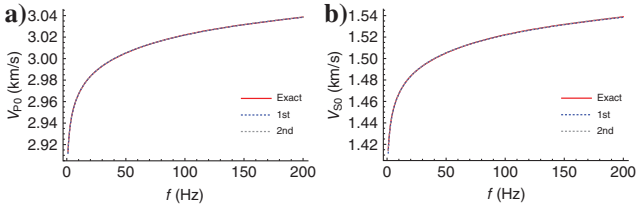

Figure 2. Frequency-dependent vertical velocities (a) V_{P0} and (b) V_{S0}. "Exact" in the legend refers to the exact values, whereas "1st" and "2nd" denote the first- and second-order approximations with respect to $\ln|f/f_0|$, respectively. On plot (a), $\tilde{V}_{P0} = 3.0$ km/s and $Q_{33} = 40$ ($\tilde{A}_{P0} = 0.0125$); on plot (b), $\tilde{V}_{S0} = 1.5$ km/s and $Q_{55} = 20$ ($\tilde{A}_{S0} = 0.025$).

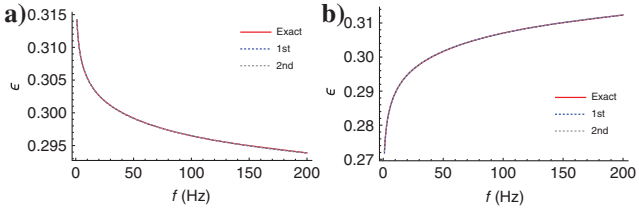

Figure 3. Variation of the Thomsen parameter ϵ with frequency for (a) model 1 and (b) model 2 from Table 1. The legend is the same as in Figure 2.

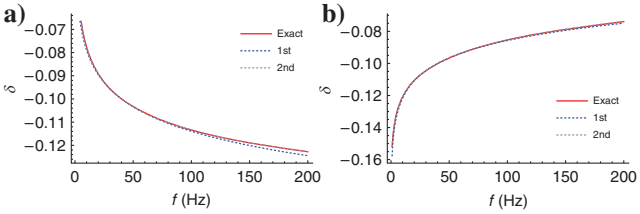

Figure 4. Same as Figure 3 but for the parameter δ.

Table 1. Medium parameters for two constant-Q VTI models at the reference frequency $f_0 = 40$ Hz.

Model	$\tilde{V}_{P0}$	$\tilde{V}_{S0}$	$\tilde{\epsilon}$	$\tilde{\delta}$	$\tilde{\gamma}$	$\tilde{A}_{P0}(Q_{33})$	$\tilde{A}_{S0}(Q_{55})$	$\tilde{\epsilon}_Q$	$\tilde{\delta}_Q$	$\tilde{\gamma}_Q$
1	3.0	1.5	0.3	−0.1	0.1	0.0125 (40)	0.0167 (30)	−0.3	−1.91	0.5
2	3.0	1.5	0.3	−0.1	0.2	0.0250 (20)	0.0333 (15)	0.3	0.98	−0.2

but it is also influenced by the parameters $\tilde{\delta}$ and $\tilde{\delta}_Q$. For the most common values of g_Q considered here, and relatively strong attenuation, the parameter δ_Q significantly varies with f, especially for low frequencies.

VISCOACOUSTIC CONSTANT-Q TRANSVERSE ISOTROPY

Simplified parameter expressions

Next, we consider the so-called "viscoacoustic" constant-Q media described by the Thomsen-type notation. The acoustic approximation is implemented by setting $\tilde{V}_{S0} = \mathcal{A}_{S0} = 0$ in equations 18, 29, and 40 (Hao and Alkhalifah, 2017, 2019). The parameters δ, η, and δ_Q then reduce to:

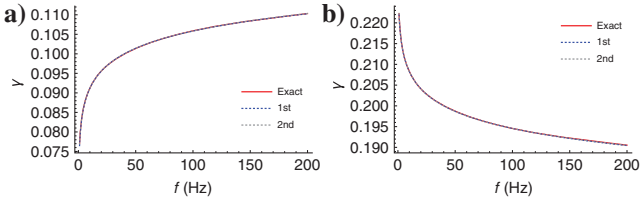

Figure 5. Same as Figure 3 but for the parameter γ.

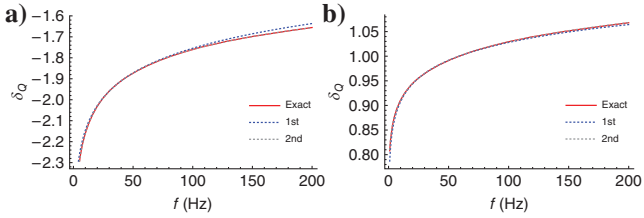

Figure 6. Frequency-dependent Thomsen-type attenuation parameter δ_Q for (a) model 1 and (b) model 2 from Table 1. The legend is the same as in Figure 2.

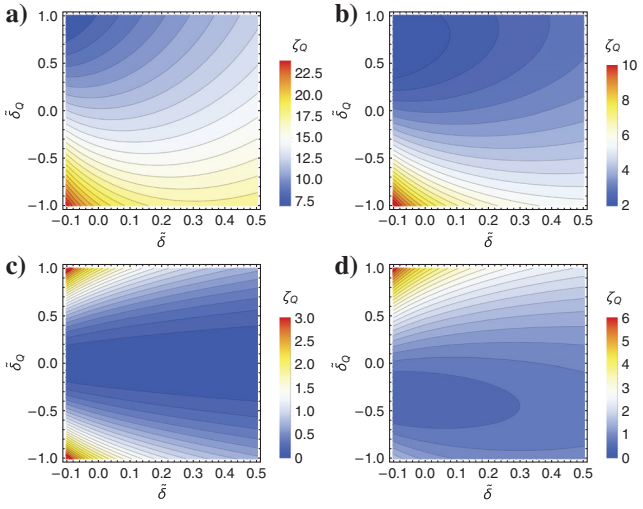

Figure 7. Contour plots of the coefficient ζ_Q as a function of $\tilde{\delta}$ and $\tilde{\delta}_Q$. The parameter $g = \tilde{V}_{S0}^2/\tilde{V}_{P0}^2 = 0.3$. The parameter $g_Q = Q_{55}^{-1}/Q_{33}^{-1}$ is set as (a) $g_Q = 3$, (b) $g_Q = 2$, (c) $g_Q = 1$, and (d) $g_Q = 0.5$.

$$\delta = \tilde{\delta} + \frac{1}{\pi} Q_{33}^{-1} \tilde{\delta}_Q \ln\left|\frac{f}{f_0}\right| + \frac{1}{\pi^2} Q_{33}^{-2} \frac{\tilde{\delta}_Q^2}{1+2\tilde{\delta}} \ln^2\left|\frac{f}{f_0}\right|, \quad (42)$$

$$\eta = \eta_0 + \frac{1}{\pi}\eta_1 Q_{33}^{-1} \ln\left|\frac{f}{f_0}\right| + \frac{1}{\pi^2}\left(\tilde{\epsilon}_Q - \frac{\tilde{\delta}_Q}{1+2\tilde{\delta}}\right)\eta_1 Q_{33}^{-2} \ln^2\left|\frac{f}{f_0}\right|, \quad (43)$$

$$\delta_Q = \tilde{\delta}_Q + \frac{2}{\pi} Q_{33}^{-1} \frac{\tilde{\delta}_Q^2}{1+2\tilde{\delta}} \ln\left|\frac{f}{f_0}\right| + \frac{2}{\pi^2} Q_{33}^{-2} \frac{\tilde{\delta}_Q^3}{(1+2\tilde{\delta})^2} \ln^2\left|\frac{f}{f_0}\right|. \quad (44)$$

Setting η (equation 43) to zero, which requires $\eta_0 = \eta_1 = 0$ (see equations 30 and 31), we obtain the elliptical conditions:

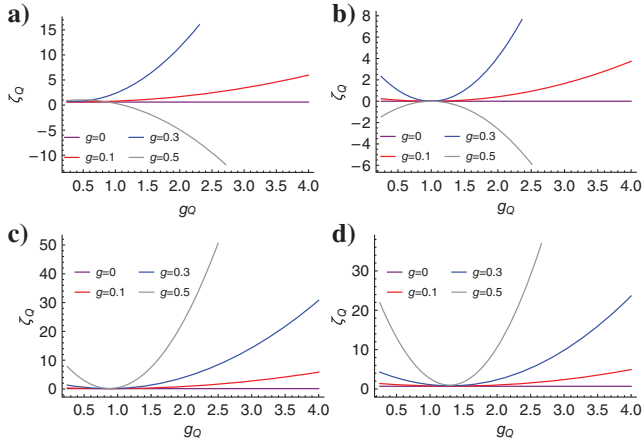

Figure 8. Variation of the coefficient ζ_Q with g_Q for different values of g: (a) $\tilde{\delta} = -0.2$ and $\tilde{\delta}_Q = -0.6$, (b) $\tilde{\delta} = -0.2$ and $\tilde{\delta}_Q = 0$, (c) $\tilde{\delta} = 0.2$ and $\tilde{\delta}_Q = -0.4$, and (d) $\tilde{\delta} = 0.2$ and $\tilde{\delta}_Q = 0.98$.

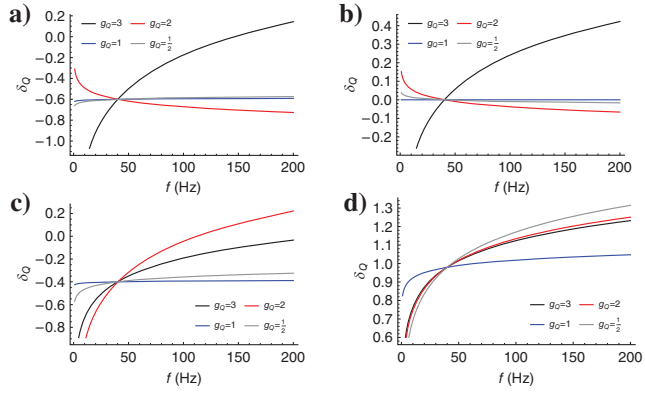

Figure 9. Variation of the attenuation parameter δ_Q with frequency for different g_Q and $g = 0.3$. The parameters $\tilde{\delta}$ and $\tilde{\delta}_Q$ are the same as in Figure 8.

DOI:10.1190/geo2022-0575.1

$$\tilde{\epsilon} = \tilde{\delta}, \tag{45}$$

$$\tilde{\epsilon}_Q = \frac{\tilde{\delta}_Q}{1 + 2\tilde{\delta}}. \tag{46}$$

Equations 45 and 46 make the parameters of viscoacoustic constant-Q media satisfy the same conditions at all frequencies:

$$\epsilon = \delta, \tag{47}$$

$$\epsilon_Q = \frac{\delta_Q}{1 + 2\delta}, \tag{48}$$

which follows from equations 17, 31, 42, and 44. Equation 47 implies that the elliptical conditions at the reference frequency ensure that $\eta = 0$ at all frequencies.

For viscoelastic constant-Q media discussed earlier, equation 47 remains approximately valid (i.e., the model is elliptical at all frequencies), if equations 45 and 46 are satisfied (see equations 29–31).

Numerical validation

Here, we verify the elliptical conditions (equations 45 and 46) by computing the anellipticity parameter η. The exact η is calculated using equations 6, 7, 11, and 12 along with equations 2 and 3 under the acoustic approximation ($\tilde{V}_{S0} = 0$ and $Q_{55}^{-1} = 0$). The first-order approximation for η is given by equation 43 without the second-order term with respect to $\ln|f/f_0|$.

Figure 10 shows that for models that satisfy equations 45 and 46 the exact anellipticity parameter is negligibly small for all frequencies (on the order of 10^{-7} for both models), which confirms that the elliptical conditions at the reference frequency lead to equation 47. In addition, our testing shows that the difference between the left and right sides of equation 48 is negligible, if equations 45 and 46 are satisfied.

PLANE-WAVE ATTENUATION IN CONSTANT-Q VTI MEDIA

In this section, we apply the obtained expressions for the Thomsen-type parameters to study the normalized plane-wave attenuation coefficients in constant-Q VTI media. The normalized phase attenuation coefficient is defined as $\mathcal{A} \equiv |\mathbf{k}_I|/|\mathbf{k}_R|$, where $\mathbf{k}_R$ and $\mathbf{k}_I$ denote the real and imaginary parts of the complex wave vector (Zhu and Tsvankin, 2006). The words "phase" and "normalized" are omitted below for brevity. The angle between $\mathbf{k}_R$ and $\mathbf{k}_I$ is called the "inhomogeneity" angle, which is not defined in plane-wave propagation (i.e., it is a free parameter that can vary within certain bounds). The coefficient $\mathcal{A}$ corresponding to $\mathbf{k}_R \| \mathbf{k}_I$ is approximately equal to the group attenuation coefficient, which can be estimated from seismic data, for a wide range of inhomogeneity angles (Behura and Tsvankin, 2009c; Tsvankin and Grechka, 2011).

Attenuation coefficients

The approximate attenuation coefficients of plane waves in viscoelastic constant-Q VTI media are given by (Zhu and Tsvankin, 2006; Tsvankin and Grechka, 2011):

$$\mathcal{A}_P = \mathcal{A}_{P0}(1 + \delta_Q \sin^2\theta \cos^2\theta + \epsilon_Q \sin^4\theta), \tag{49}$$

$$\mathcal{A}_{SV} = \mathcal{A}_{S0}(1 + \sigma_Q \sin^2\theta \cos^2\theta), \tag{50}$$

$$\mathcal{A}_{SH} = \mathcal{A}_{S0}(1 + \gamma_Q \sin^2\theta), \tag{51}$$

where the subscripts P, SV, and SH denote the wave types and θ is the phase angle measured from the vertical. The quantity σ_Q in equation 50 is defined as (Zhu and Tsvankin, 2006):

$$\sigma_Q = 2\frac{V_{P0}^2}{V_{S0}^2}\left(\frac{Q_{55}}{Q_{33}} - 1\right)(\epsilon - \delta) + \frac{V_{P0}^2 Q_{55}}{V_{S0}^2 Q_{33}}(\epsilon_Q - \delta_Q). \tag{52}$$

Equations 49–51 are derived under the assumption of weak attenuation and weak anisotropy (in both velocity and attenuation). Note that the effective quality factor, assumed to be frequency-independent in constant-Q TI media, is proportional to the inverse of the attenuation coefficient (Zhu and Tsvankin, 2006).

Substitution of the Thomsen parameters from equations 15–19 and 36–40 into equations 49–52 allows us to separate the frequency-dependent parts of the attenuation coefficients. The approximate P-wave attenuation coefficient then becomes (only the linear term in $\ln|f/f_0|$ is retained):

$$\mathcal{A}_P = \tilde{\mathcal{A}}_{P0}\left(1 + \tilde{\delta}_Q \sin^2\theta \cos^2\theta + \tilde{\epsilon}_Q \sin^4\theta + R_P \ln\left|\frac{f}{f_0}\right|\right), \tag{53}$$

where R_P controls the derivative of $\mathcal{A}_P$ with respect to $\ln|f/f_0|$,

$$R_P = \frac{1}{\pi}\tilde{\mathcal{A}}_{P0}\zeta_Q \sin^2(2\theta), \tag{54}$$

and ζ_Q is defined in equation 22.

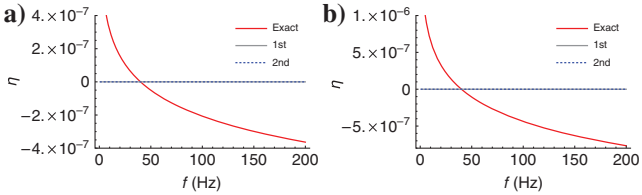

Figure 10. Variation of the anellipticity parameter η with frequency under the elliptical conditions (equations 45 and 46). The P-wave quality factor and reference vertical velocity at $f_0 = 40$ Hz are $Q_{33} = 40$ and $\tilde{V}_{P0} = 3$ km/s. The parameters $\tilde{\epsilon}$ and $\tilde{\epsilon}_Q$ are (a) $\tilde{\epsilon} = 0.3$ and $\tilde{\epsilon}_Q = -0.33$ and (b) $\tilde{\epsilon} = 0.2$ and $\tilde{\epsilon}_Q = 0.4$. The legend is the same as in Figure 2.

For SV-waves,

$$\mathcal{A}_{\rm SV} = \tilde{\mathcal{A}}_{\rm S0}\left(1 + \tilde{\sigma}_Q \sin^2\theta\cos^2\theta + R_{\rm SV}\ln\left|\frac{f}{f_0}\right|\right), \quad (55)$$

with

$$\tilde{\sigma}_Q = \frac{2}{g}\left(\frac{1}{g_Q} - 1\right)(\tilde{\epsilon} - \tilde{\delta}) + \frac{1}{g g_Q}(\tilde{\epsilon}_Q - \tilde{\delta}_Q), \quad (56)$$

$$R_{\rm SV} = \frac{1}{\pi}\tilde{\mathcal{A}}_{\rm S0}\,\sigma'_Q \sin^2(2\theta), \quad (57)$$

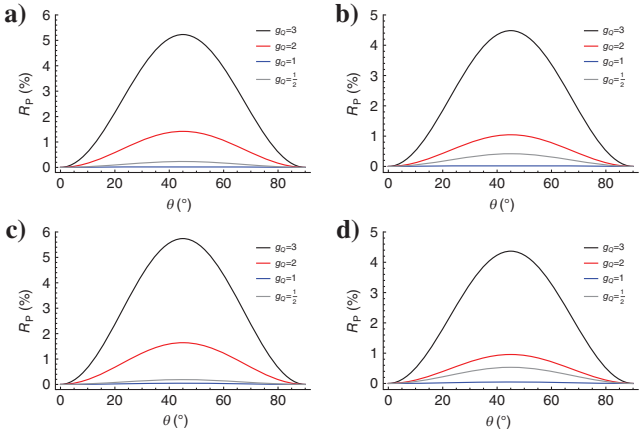

Figure 11. Variation of the P-wave dispersion factor $R_{\rm P}$ (equation 54) with the phase angle for different g_Q. The reference parameters defined at $f_0 = 40$ Hz are $\tilde{V}_{\rm P0} = 3.0$ km/s, $g = 0.3$, $\tilde{\epsilon} = 0.2$, $\tilde{\mathcal{A}}_{\rm P0} = 0.0125$ (corresponding to $Q_{33} = 40$), and $\tilde{\epsilon}_Q = -0.1$: (a) $\tilde{\delta} = 0.1$ and $\tilde{\delta}_Q = -0.2$, (b) $\tilde{\delta} = 0.1$ and $\tilde{\delta}_Q = 0.2$, (c) $\tilde{\delta} = -0.1$ and $\tilde{\delta}_Q = -0.2$, and (d) $\tilde{\delta} = -0.1$ and $\tilde{\delta}_Q = 0.2$.

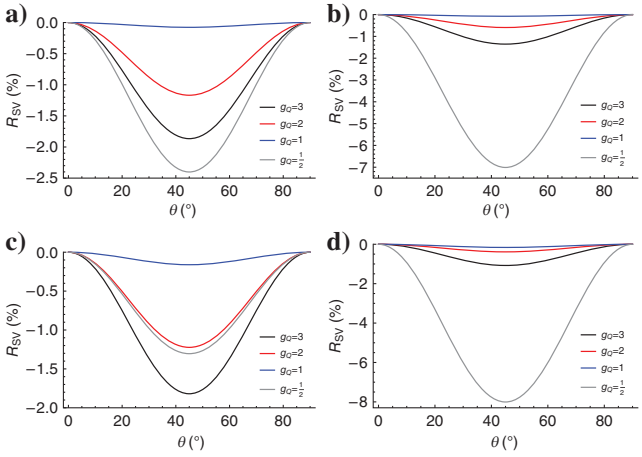

Figure 12. Variation of the SV-wave dispersion factor $R_{\rm SV}$ (equation 57) with the phase angle for different g_Q. The reference parameters defined at $f_0 = 40$ Hz are $\tilde{V}_{\rm P0} = 3.0$ km/s, $g = 0.3$, $\tilde{\epsilon} = 0.2$, $\tilde{\mathcal{A}}_{\rm S0} = 0.0125$ (corresponding to $Q_{55} = 40$), $\tilde{\epsilon}_Q = -0.1$. The parameters $\tilde{\delta}$ and $\tilde{\delta}_Q$ are the same as in Figure 11.

$$\sigma'_Q = \frac{2(1-g_Q)}{g g_Q^2}[(1-g_Q)(\tilde{\epsilon} - \tilde{\delta}) - \tilde{\delta}_Q + (1+\tilde{\epsilon})\tilde{\epsilon}_Q] - \frac{\zeta_Q}{g g_Q^2}, \quad (58)$$

where g and g_Q are given by equations 27 and 23, respectively. The factor $R_{\rm SV}$ controls the derivative of $\mathcal{A}_{\rm SV}$ with respect to $\ln|f/f_0|$.

The terms $\tilde{\mathcal{A}}_{\rm P0}\,R_{\rm P}$ and $\tilde{\mathcal{A}}_{\rm S0}\,R_{\rm SV}$ define the rate of the P- and SV-wave attenuation-coefficient change (increase or decrease) with respect to $\ln|f/f_0|$. The larger $R_{\rm P}$ and $R_{\rm SV}$ are, the stronger is the dispersion (frequency dependence) of $\mathcal{A}_{\rm P}$ and $\mathcal{A}_{\rm SV}$. Therefore, $R_{\rm P}$ and $R_{\rm SV}$ can be called the P- and SV-wave "dispersion factors," respectively.

The SH-wave attenuation coefficient (equation 51) is independent of frequency, with $\gamma_Q = \tilde{\gamma}_Q$:

$$\mathcal{A}_{\rm SH} = \tilde{\mathcal{A}}_{\rm S0}(1 + \tilde{\gamma}_Q \sin^2\theta). \quad (59)$$

Numerical dispersion analysis

Here, we evaluate the frequency dependence of the attenuation coefficients of P- and SV-waves, starting with the dispersion factors $R_{\rm P}$ and $R_{\rm SV}$ (equations 54 and 57). As before, we restrict g_Q to the realistic range $0.5 < g_Q \le 3$ (Figure 1). Figures 11 and 12 show that $g_Q = 1$ yields the smallest values of $R_{\rm P}$ and $R_{\rm SV}$; the dispersion factors and the magnitude of their variation with angle increase with the deviation of g_Q from unity.

Next, we use the medium parameters from Figures 11d and 12d to calculate the exact attenuation coefficients for P- and SV-waves (respectively) at three frequencies. For the reference frequency $f_0 = 40$ Hz, the term $\ln|f/f_0|$ in equations 54 and 57 is close to -1 at $f = 15$ Hz and 1 at $f = 109$ Hz. In agreement with equations 53 and 55, the variation of $\mathcal{A}_{\rm P}$ with $\ln|f/f_0|$ between 15 and 40 Hz (and 40 and 109 Hz) is approximately proportional to $R_{\rm P}$, and the corresponding variation of $\mathcal{A}_{\rm SV}$ is approximately proportional to $R_{\rm SV}$.

Figures 13 and 14 show that the frequency dependence of the P- and SV-wave attenuation coefficients $\mathcal{A}_{\rm P}$ and $\mathcal{A}_{\rm SV}$ is generally mild.

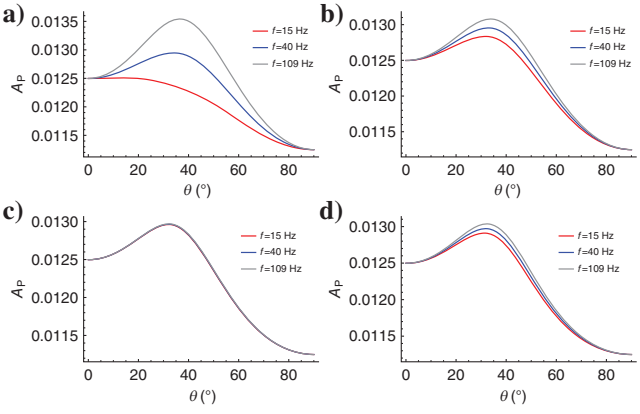

Figure 13. Variation of the P-wave attenuation coefficient with the phase angle at different frequencies. The medium parameters are the same as in Figure 11d: (a) $g_Q = 3$, (b) $g_Q = 2$, (c) $g_Q = 1$, and (d) $g_Q = 0.5$.

However, it may become noticeable for propagation angles close to 45°, as illustrated in Figures 15 and 16. Here, $\mathcal{A}_P$ and $\mathcal{A}_{SV}$ exhibit a more significant variation with frequency for strongly attenuative media ($Q_{33} = Q_{55} = 20$) when $g_Q \geq 2$ (for P-waves) and $g_Q \leq 0.5$ (for SV-waves).

DISCUSSION

Our analytic approximations for the Thomsen-type parameters of constant-Q TI media provide an explicit relationship between these parameters and frequency. As a consequence, the frequency dependence of the attenuation coefficients can be conveniently studied for the entire range of propagation angles. Our analysis shows that the P- and SV-wave attenuation coefficients and quality factors for constant-Q media do depend on frequency, although that dependence may not be significant for weak attenuation (see equations 53 and 55). Note that the proposed formulas for the attenuation coefficients remain entirely valid for TTI media, if the phase angle θ is defined with respect to the symmetry axis.

In addition, the obtained approximate Thomsen-type parameters could be used to derive other useful formulas for constant-Q TI media. For example, the substitution of these approximations into the linearized reflection coefficients for general attenuative TI media (Behura and Tsvankin, 2009b) should yield the corresponding expressions for constant-Q TI models.

Because our parameter approximations are derived using a series expansion with respect to $\ln|\omega/\omega_0|$ (or $\ln|f/f_0|$), their accuracy decreases as ω deviates from the reference angular frequency ω_0, which has to be taken into account for strongly attenuative media.

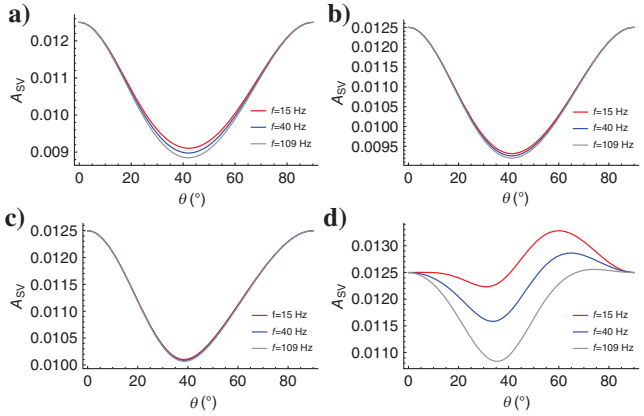

Figure 14. Variation of the SV-wave attenuation coefficient with the phase angle at different frequencies. The medium parameters are the same as in Figure 12d: (a) $g_Q = 3$, (b) $g_Q = 2$, (c) $g_Q = 1$, and (d) $g_Q = 0.5$.

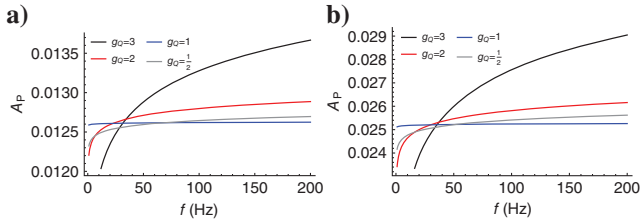

Figure 15. Variation of the P-wave attenuation coefficient with frequency at $\theta = 45°$ for different g_Q. Except for $\tilde{\mathcal{A}}_{P0}$, the medium parameters are the same as in Figures 11d and 13. On plot (a), $\tilde{\mathcal{A}}_{P0} = 0.0125$ (corresponding to $Q_{33} = 40$); on plot (b), $\tilde{\mathcal{A}}_{P0} = 0.025$ (corresponding to $Q_{33} = 20$).

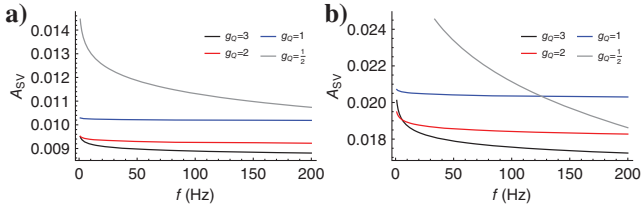

Figure 16. Variation of the SV-wave attenuation coefficient with frequency at $\theta = 45°$ for different g_Q. Except for $\tilde{\mathcal{A}}_{S0}$, the medium parameters are the same as in Figures 12d and 14. On plot (a), $\tilde{\mathcal{A}}_{S0} = 0.0125$ (corresponding to $Q_{55} = 40$); on plot (b), $\tilde{\mathcal{A}}_{S0} = 0.025$ (corresponding to $Q_{55} = 20$).

CONCLUSIONS

We have obtained concise analytic expressions for the Thomsen-type parameters of constant-Q TI media. All Thomsen velocity parameters (V_{P0}, V_{S0}, ϵ, δ, and γ) are frequency dependent, with the reference attenuation parameters $\tilde{\mathcal{A}}_{P0}$ (proportional to $1/Q_{33}$) and $\tilde{\mathcal{A}}_{S0}$ (proportional to $1/Q_{55}$) controlling the dispersion (frequency variation) of the vertical velocities V_{P0} and V_{S0}, respectively. The reference attenuation parameters $\tilde{\epsilon}_Q$, $\tilde{\delta}_Q$, and $\tilde{\gamma}_Q$ govern the variation of the anisotropy parameters ϵ, δ, and γ with frequency. However, the frequency dependence of all Thomsen velocity parameters is weak in a wide frequency range, even for strong attenuation. In viscoacoustic constant-Q TI media, the elliptical conditions at the reference frequency ensure that the anellipticity parameter η vanishes for all frequencies.

Despite the fact that all Q_{ij} elements in constant-Q TI media are frequency independent, one of the Thomsen-type attenuation parameters (δ_Q) does vary with frequency. The frequency dependence of δ_Q is controlled by the newly defined coefficient ζ_Q and can be substantial when ζ_Q has a large magnitude. As a result, the frequency variation of the P- and SV-wave attenuation coefficients may be nonnegligible at oblique propagation angles with the symmetry axis. That variation is strongly dependent on the ratio of the vertical quality factors $g_Q = Q_{33}/Q_{55}$. Both attenuation coefficients are insensitive to frequency for $g_Q = 1$, whereas their frequency dependence is most substantial for $g_Q \geq 3$ (for P-waves) and $g_Q \leq 0.5$ (for SV-waves). In contrast, the SH-wave attenuation coefficient in constant-Q TI media is frequency-independent.

The constant-Q assumption is often made in attenuation analysis because the effective attenuation coefficients estimated from seismic data (e.g., using the spectral-ratio method) become linear functions of frequency. However, our results show that this linear dependence may not hold for constant-Q TI models, which can cause errors in the inversion for the attenuation parameters.

ACKNOWLEDGMENTS

We would like to express our gratitude to the associate editor and the anonymous reviewers for their constructive feedback. I. Tsvankin acknowledges the support of the Consortium Project on Seismic

Inverse Methods for Complex Structures at the Center for Wave Phenomena (CWP), Colorado School of Mines.

DATA AND MATERIALS AVAILABILITY

Data associated with this research are available and can be obtained by contacting the corresponding author.

APPENDIX A

COMPLEX STIFFNESS COEFFICIENTS EXPRESSED IN TERMS OF THE THOMSEN-TYPE PARAMETERS

The stiffness coefficients for the constant-Q attenuative VTI model (equations 1–3) can be found at the reference frequency as $M_{ij}|_{f=f_0} = \tilde{M}_{ij}^R(1 - i/Q_{ij})$. Using the parameter definitions in equations 4–12, we express $\tilde{M}_{ij}^R$ and Q_{ij} in terms of the reference Thomsen-type parameters as follows (Tsvankin, 1997; Zhu and Tsvankin, 2006; Tsvankin and Grechka, 2011):

$$\tilde{M}_{33}^R = \rho\tilde{V}_{P0}^2, \tag{A-1}$$

$$\tilde{M}_{55}^R = \rho\tilde{V}_{S0}^2, \tag{A-2}$$

$$\tilde{M}_{11}^R = \rho\tilde{V}_{P0}^2(1 + 2\tilde{\epsilon}), \tag{A-3}$$

$$\tilde{M}_{66}^R = \rho\tilde{V}_{S0}^2(1 + 2\tilde{\gamma}), \tag{A-4}$$

$$\tilde{M}_{13}^R = -\rho\tilde{V}_{S0}^2 + \rho\sqrt{(\tilde{V}_{P0}^2 - \tilde{V}_{S0}^2)[(1 + 2\tilde{\delta})\tilde{V}_{P0}^2 - \tilde{V}_{S0}^2]}, \tag{A-5}$$

$$Q_{33}^{-1} = \frac{2\tilde{\mathcal{A}}_{P0}}{1 - \tilde{\mathcal{A}}_{P0}^2}, \tag{A-6}$$

$$Q_{55}^{-1} = \frac{2\tilde{\mathcal{A}}_{S0}}{1 - \tilde{\mathcal{A}}_{S0}^2}, \tag{A-7}$$

$$Q_{11}^{-1} = Q_{33}^{-1}(1 + \tilde{\epsilon}_Q), \tag{A-8}$$

$$Q_{66}^{-1} = Q_{55}^{-1}(1 + \tilde{\gamma}_Q), \tag{A-9}$$

$$Q_{13}^{-1} = Q_{33}^{-1}(1 + \tilde{\delta}_Q f_1 + f_2) - Q_{55}^{-1} f_2, \tag{A-10}$$

with

$$f_1 = \frac{\tilde{M}_{33}^R(\tilde{M}_{33}^R - \tilde{M}_{55}^R)}{2\tilde{M}_{13}^R(\tilde{M}_{13}^R + \tilde{M}_{55}^R)}, \tag{A-11}$$

$$f_2 = \frac{\tilde{M}_{55}^R(\tilde{M}_{13}^R + \tilde{M}_{33}^R)^2}{2\tilde{M}_{13}^R(\tilde{M}_{13}^R + \tilde{M}_{55}^R)(\tilde{M}_{33}^R - \tilde{M}_{55}^R)}. \tag{A-12}$$

APPENDIX B

EXPLICIT EXPRESSIONS FOR S_N

Here, we provide explicit expressions for the coefficients s_n in equation 41.

The coefficient s_0 is given by:

$$s_0 = \frac{g(1 - g + \chi)^2(h_0 + h_1 g + h_2 g^2 + h_3 g^3 + h_4 g^4 + h_5 g^5)}{(1 - g)^3\chi^3(g - \chi)^2}, \tag{B-1}$$

where

$$h_0 = -(1 + 2\tilde{\delta})^2\chi, \tag{B-2}$$

$$h_1 = (1 + 2\tilde{\delta})(5 + 10\tilde{\delta} + 2\chi), \tag{B-3}$$

$$h_2 = (1 + 2\tilde{\delta})[2(\tilde{\delta} - 3)\chi - 13\tilde{\delta} - 14], \tag{B-4}$$

$$h_3 = \tilde{\delta}(7\tilde{\delta} + 9\chi + 30) + 7\chi + 15, \tag{B-5}$$

$$h_4 = -\tilde{\delta}^2 - 2(\tilde{\delta} + 1)\chi - 11\tilde{\delta} - 8, \tag{B-6}$$

$$h_5 = 2(1 + \tilde{\delta}). \tag{B-7}$$

For the coefficient s_1, we have:

$$s_1 = \frac{3g(g - \chi - 1)(k_0 + k_1 g + k_2 g^2 + k_3 g^3 + k_4 g^4)}{2(1 - g)\chi^3(g - \chi)^2}, \tag{B-8}$$

where

$$k_0 = -2(1 + 2\tilde{\delta})^2, \tag{B-9}$$

$$k_1 = 2[1 + \chi + 4\tilde{\delta}(\tilde{\delta} + \chi + 1)], \tag{B-10}$$

$$k_2 = 2(\chi + 1) - \tilde{\delta}(\chi + 3), \tag{B-11}$$

$$k_3 = -(\tilde{\delta} + 2\chi + 4), \tag{B-12}$$

$$k_4 = 2. \tag{B-13}$$

Finally, the coefficient s_2 has the form:

$$s_2 = \frac{3g[3 + 6\tilde{\delta} + 2\chi - 3g(3\tilde{\delta} + 2\chi + 3) + 3g^2(\tilde{\delta} + \chi + 3) - 3g^3]}{2\chi^3(g - \chi)^2}, \tag{B-14}$$

$$s_3 = \frac{(1 - g)^2(4\chi - 3g)}{4\chi^3(g - \chi)^2}. \tag{B-15}$$

The quantities g and χ are defined in equations 27 and 28, respectively.

REFERENCES

Alkhalifah, T., and I. Tsvankin, 1995, Velocity analysis for transversely isotropic media: Geophysics, **60**, 1550–1566, doi: 10.1190/1.1443888.

Bai, T., and I. Tsvankin, 2016, Time-domain finite-difference modeling for attenuative anisotropic media: Geophysics, **81**, no. 2, C69–C77, doi: 10.1190/geo2015-0424.1.

Barton, N., 2006, Rock quality, seismic velocity, attenuation and anisotropy: CRC Press.

Behura, J., and I. Tsvankin, 2009a, Estimation of interval anisotropic attenuation from reflection data: Geophysics, **74**, no. 6, A69–A74, doi: 10.1190/1.3191733.

Behura, J., and I. Tsvankin, 2009b, Reflection coefficients in attenuative anisotropic media: Geophysics, **74**, no. 5, WB193–WB202, doi: 10.1190/1.3142874.

Behura, J., and I. Tsvankin, 2009c, Role of the inhomogeneity angle in anisotropic attenuation analysis: Geophysics, **74**, no. 5, WB177–WB191, doi: 10.1190/1.3148439.

Behura, J., I. Tsvankin, E. Jenner, and A. Calvert, 2012, Estimation of interval velocity and attenuation anisotropy from reflection data at coronation field: The Leading Edge, **31**, 580–587, doi: 10.1190/tle31050580.1.

Best, A. I., J. Sothcott, and C. McCann, 2007, A laboratory study of seismic velocity and attenuation anisotropy in near-surface sedimentary rocks: Geophysical Prospecting, **55**, 609–625, doi: 10.1111/j.1365-2478.2007.00642.x.

Carcione, J. M., 1997a, Reflection and refraction of antiplane shear waves at a plane boundary between viscoelastic anisotropic media: Proceedings of the Royal Society of London. Series A: Mathematical, Physical and Engineering Sciences, **453**, 919–942, doi: 10.1098/rspa.1997.0051.

Carcione, J. M., 1997b, Reflection and transmission of qP-qS plane waves at a plane boundary between viscoelastic transversely isotropic media: Geophysical Journal International, **129**, 669–680, doi: 10.1111/j.1365-246X.1997.tb04502.x.

Carcione, J. M., 2014, Wave fields in real media: Theory and numerical simulation of wave propagation in anisotropic, anelastic, porous and electromagnetic media: Handbook of geophysical exploration, 3rd ed.: Elsevier.

Červený, V., and I. Pšencík, 2005a, Plane waves in viscoelastic anisotropic media — I. Theory: Geophysical Journal International, **161**, 197–212, doi: 10.1111/j.1365-246X.2005.02589.x.

Červený, V., and I. Pšencík, 2005b, Plane waves in viscoelastic anisotropic media — II. Numerical examples: Geophysical Journal International, **161**, 213–229, doi: 10.1111/j.1365-246X.2005.02590.x.

Červený, V., and I. Pšencík, 2009, Perturbation Hamiltonians in heterogeneous anisotropic weakly dissipative media: Geophysical Journal International, **178**, 939–949, doi: 10.1111/j.1365-246X.2009.04218.x.

Hao, Q., and T. Alkhalifah, 2017, An acoustic eikonal equation for attenuating transversely isotropic media with a vertical symmetry axis: Geophysics, **82**, no. 1, C9–C20, doi: 10.1190/geo2016-0160.1.

Hao, Q., and T. Alkhalifah, 2019, Viscoacoustic anisotropic wave equations: Geophysics, **84**, no. 6, C323–C337, doi: 10.1190/geo2018-0865.1.

Hao, Q., and S. Greenhalgh, 2021, Nearly constant Q models of the generalized standard linear solid type and the corresponding wave equations: Geophysics, **86**, no. 4, T239–T260, doi: 10.1190/geo2020-0548.1.

Hao, Q., S. Greenhalgh, X. Huang, and H. Li, 2022, Viscoelastic wave propagation for nearly constant Q transverse isotropy: Geophysical Prospecting, **70**, 1176–1192, doi: 10.1111/1365-2478.13230.

Kjartansson, E., 1979, Constant Q-wave propagation and attenuation: Journal of Geophysical Research, **84**, 4737–4748, doi: 10.1029/JB084iB09p04737.

Kolsky, H., 1956, The propagation of stress pulses in viscoelastic solids: Philosophical Magazine, **1**, 693–710, doi: 10.1080/14786435608238144.

Li, H., S. Greenhalgh, S. Chen, X. Liu, and B. Liu, 2020, A robust Q estimation scheme for adaptively handling asymmetric wavelet spectrum variations in strongly attenuating media: Geophysics, **85**, no. 4, V345–V354, doi: 10.1190/geo2019-0442.1.

Shekar, B., and I. Tsvankin, 2011, Estimation of shear-wave interval attenuation from mode-converted data: Geophysics, **76**, no. 6, D11–D19, doi: 10.1190/geo2010-0415.1.

Shekar, B., and I. Tsvankin, 2012, Anisotropic attenuation analysis of cross-hole data generated during hydraulic fracturing: The Leading Edge, **31**, 588–593, doi: 10.1190/tle31050588.1.

Shekar, B., and I. Tsvankin, 2014, Point-source radiation in attenuative anisotropic media: Geophysics, **79**, no. 5, WB25–WB34, doi: 10.1190/geo2013-0417.1.

Thomsen, L., 1986, Weak elastic anisotropy: Geophysics, **51**, 1954–1966, doi: 10.1190/1.1442051.

Tsvankin, I., 1997, Anisotropic parameters and P-wave velocity for orthorhombic media: Geophysics, **62**, 1292–1309, doi: 10.1190/1.1444231.

Tsvankin, I., 2001, Seismic signatures and analysis of reflection data in anisotropic media: Elsevier Science Ltd.

Tsvankin, I., and V. Grechka, 2011, Seismology of azimuthally anisotropic media and seismic fracture characterization: SEG.

Vavryčuk, V., 2008, Real ray tracing in anisotropic viscoelastic media: Geophysical Journal International, **175**, 617–626, doi: 10.1111/j.1365-246X.2008.03898.x.

Vavryčuk, V., 2007a, Asymptotic Green's function in homogeneous anisotropic viscoelastic media: Proceedings of the Royal Society A: Mathematical, Physical and Engineering Sciences, **463**, 2689–2707, doi: 10.1098/rspa.2007.1862.

Vavryčuk, V., 2007b, Ray velocity and ray attenuation in homogeneous anisotropic viscoelastic media: Geophysics, **72**, no. 6, D119–D127, doi: 10.1190/1.2768402.

Zhang, C., and T. J. Ulrych, 2002, Estimation of quality factors from CMP records: Geophysics, **67**, 1542–1547, doi: 10.1190/1.1512799.

Zhu, Y., and I. Tsvankin, 2006, Plane-wave propagation in attenuative transversely isotropic media: Geophysics, **71**, no. 2, T17–T30, doi: 10.1190/1.2187792.

Zhu, Y., I. Tsvankin, P. Dewangan, and K. van Wijk, 2007, Physical modeling and analysis of P-wave attenuation anisotropy in transversely isotropic media: Geophysics, **72**, no. 1, D1–D7, doi: 10.1190/1.2374797.

Zhubayev, A., M. E. Houben, D. M. Smeulders, and A. Barnhoorn, 2016, Ultrasonic velocity and attenuation anisotropy of shales, Whitby, United Kingdom: Geophysics, **81**, no. 1, D45–D56, doi: 10.1190/geo2015-0211.1.

Ilya Tsvankin received an M.S. (1978) and a Ph.D. (1982) in geophysics from Moscow State University in Russia. From 1978 to 1989, he worked at the Institute of Physics of the Earth in Moscow and was deputy head of laboratory "Geophysics of Anisotropic Media." After moving to the United States in 1990, he became a consultant to the Amoco Production Research Center in Tulsa. Since 1992, he has been on the faculty of Colorado School of Mines, where he is currently a professor in geophysics and director of the CWP. He received the Virgil Kauffman Gold Medal Award from SEG for his work in seismic anisotropy in 1996. His other recognitions are the SEG Best Paper in Geophysics Award (2009), election to Fellowship of the

Institute of Physics (2011), SEG Honorary Membership Award (2015), and SEG Outstanding Educator Award (2020). The third edition of his widely used monograph "Seismic signatures and analysis of reflection data in anisotropic media" was published by SEG in 2012. He also coauthored (with Vladimir Grechka) the book *Seismology of azimuthally anisotropic media and seismic fracture characterization* (SEG, 2011). His research interests include seismic modeling, inversion, and processing for anisotropic media; fracture characterization; time-lapse seismic; and nonlinear elasticity.

DOI:10.1190/geo2022-0575.1